$[Mn(bpm)(N_3)_2]_n$: A One-Dimensional Coordination Polymer Exhibiting Strong Ferromagnetic−Antiferromagnetic Alternating Interactions

Liang-Fu Tang,* Lei Zhang, Li-Chun Li, Peng Cheng,* Zhi-Hong Wang, and Ji-Tao Wang

Department of Chemistry, Nankai University, Tianjin 300071, P. R. China

Received July 26, 1999

Introduction

The structural and magnetic properties of binuclear and polymetallic complexes with azido-bridged ligands have received considerable attention in the past three decades.[1] From the magnetic point of view, the most interesting characteristic of azido-bridged complexes is that the azido ligand is a very effective superexchange pathway for its two main coordination modes and very effectively forms binuclear,[2] tetranuclear,[3] and one-,[4] two-,[5] and three-dimensional[6] complexes, some of which show spontaneous magnetization at T_c between 16 and 40 K.[7] Exchange interactions between manganese(II) ions propagated through azido bridges are strongly dependent on the bridging modes of the N_3^- ion. As is well-known, the azido ligand stabilizes either end-on or end-to-end coordination models when it links two manganese centers, giving ferro- or antiferromagnetic interactions, respectively, subject to certain restrictions on bond angles, torsion angles, and Mn−N bond distances. Specific magneto−structural correlations have been developed by Ruiz on the basis of hybrid density functional theory (DFT) methods[8] and by Rojo on the basis of extended Hückel molecular orbital (EHMO) calculations.[4a] The results are somewhat different for the values of the Mn−N−Mn angles, which cause a crossover from ferro- to antiferromagnetism.

Table 1. Crystallographic Data for $[Mn(bpm)(N_3)_2]_n$

empirical formula	$C_{14}H_{16}Mn_2N_{20}$
a, Å	7.590(2)
b, Å	8.924(2)
c, Å	16.961(3)
α, deg	90
β, deg	93.98(3)
γ, deg	90
V, Å^3	1146(1)
Z	2
fw	574.29
space group	$P2_1/n$ (No. 14)
T, K	299 ± 1
λ(Mo Kα), Å	0.710 73
ρ_{calcd}, g·cm^{-3}	1.664
μ(Mo Kα), mm^{-1}	1.1062
R^a	0.040
$R_w{}^b$	0.049

^{a} $R = \sum(|F_o| - |F_c|)/\sum F_o$. ^{b} $R_w = [\sum w(|F_o| - |F_c|)^2/\sum wF_o{}^2]^{1/2}$; $w^{-1} = \sigma^2(F) + 0.0001F^2$.

With the purpose of examining and investigating further magnetic interactions as a function of a one-dimensional chain complex, we succeeded in synthesizing the one-dimensional complex $[Mn(bpm)(N_3)_2]_n$, in which bpm is bis(pyrazol-1-yl)-methane. Magnetic measurements indicate that, in agreement with the structural data, the chain shows a regular alternation of ferromagnetic and antiferromagnetic interactions and shows antiferromagnetic interactions in the interchains.

Experimental Section

Preparation of $[Mn(bpm)(N_3)_2]_n$. A methanol solution of bpm (0.148 g, 1.0 mmol) was added dropwise to a mixture of manganese perchlorate hexahydrate (0.362 g, 1.0 mmol) and sodium azide (0.137 g, 2.1 mmol) in water−methanol (1:2, 20 mL). The final clear solution was kept at room temperature for 5 days to produce the complex as well-formed light-yellow crystals of $[Mn(bpm)(N_3)_2]_n$, suitable for X-ray determination. Yield: ca. 72%. Anal. Calcd for $C_{14}H_{16}Mn_2N_{20}$: C, 29.28; H, 2.81; N, 48.78; Mn, 19.13. Found: C, 29.42; H, 3.02; N, 48.40; Mn, 18.97.

Crystallographic Data Collection and Refinement of the Structure. The X-ray data for a single-crystal of $[Mn(bpm)(N_3)_2]_n$ having the approximate dimensions 0.30 × 0.35 × 0.40 mm were collected on an Enraf-Nonius CAD4 diffractometer equipped with graphite-monochromated Mo Kα (λ = 0.710 73 Å) radiation at room temperature. The crystallographic data, conditions restrained for the intensity data collection, and some features of the structure refinement are listed in Table 1. An $\omega-2\theta$ scan mode was employed for collection of data in the range $4.5° \le \theta \le 25°$. A total of 2211 reflections was collected, and 1855 independent reflections (R_{int} = 0.035) were considered for use in the succeeding refinement. The data were corrected for Lorentz−polarization and absorption effects (DIFABS[9]). The structures were solved by direct methods and refined by full-matrix least-squares methods on *F* using the SHELXTL-PC computer program package.[10] All non-hydrogen atoms were refined anisotropically. Hydrogen atoms were located on calculated positions. The final refinement including hydrogen atoms converged to R = 0.040 and R_w = 0.049. The number of refined parameters was 153. Maximum and minimum peaks in the final difference Fourier synthesis were 0.60 and −0.37 e·Å^{-3}. Final atomic coordinates are reported in Table 2, and significant bond parameters are given in Table 3.

(1) (a) Bonner, J. In *Magneto-Structural Correlations in Exchange Coupled Systems*; Willet, R. D., Gatteschi, D., Kahn, O., Eds.; NATO ASI Series 140; Reidel: Dordrecht, The Netherlands, 1985; p 17. (b) Rabis, J.; Monfort, M.; Solans, X.; Drillon, M. *Inorg. Chem.* **1994**, *33*, 742. (c) Sikorav, S.; Bkouche-Waksman, I.; Kahn, O. *Inorg. Chem.* **1984**, *23*, 490. (d) Thompson, L. K.; Tandon, S. S.; Manuel, M. E. *Inorg. Chem.* **1995**, *34*, 2356.

(2) (a) Rabis, J.; Monfort, M.; Diaz, C.; Bastos, C.; Solans, X. *Inorg. Chem.* **1994**, *33*, 484. (b) Cortés, R.; Pizarro, L.; Lezama, L.; Arriortua, M. S.; Rojo, T. *Inorg. Chem.* **1994**, *33*, 2697.

(3) (a) Rabis, J.; Monfort, M.; Costa, R.; Solans, X. *Inorg. Chem.* **1993**, *32*, 695. (b) Halcrow, M. C.; Sun, J.-S.; Huffman, J. C.; Christou, G. *Inorg. Chem.* **1995**, *34*, 4167.

(4) (a) Cortés, R.; Drillon, M.; Solans, X.; Lezama, L.; Rojo, T. *Inorg. Chem.* **1997**, *36*, 677. (b) Cortés, R.; Lezama, L.; Pizarro, L.; Arriortua, M. S.; Solans, X.; Rojo, T. *Angew. Chem., Int. Ed. Engl.* **1994**, *33*, 2488. (c) Escuer, A.; Vicente, R.; Goher, M. A. S.; Mautner, F. A. *Inorg. Chem.* **1998**, *37*, 782. (d) Viau, G.; Lombardi, M. G.; Munno, G. D.; Julve, M.; Floret, F.; Faus, J.; Caneschi, A.; Clemente-Juan, J. M. *J. Chem. Soc., Chem. Commun.* **1997**, 1195.

(5) Mautner, F. A.; Cortés, R.; Lezama, L.; Rojo, T. *Angew. Chem., Int. Ed. Engl.* **1995**, *35*, 78.

(6) (a) Escuér, A.; Vicente, R.; Goher, M. A. S.; Mautner, F. A. *Inorg. Chem.* **1995**, *34*, 5707. (b) Escuér, A.; Vicente, R.; Goher, M. A. S.; Mautner, F. A. *Inorg. Chem.* **1996**, *35*, 6386. (c) Escuér, A.; Vicente, R.; Goher, M. A. S.; Mautner, F. A. *J. Chem. Soc., Dalton Trans.* **1997**, 4431.

(7) Escuér, A.; Vicente, R.; Goher, M. A. S.; Mautner, F. A. *Inorg. Chem.* **1997**, *36*, 3440.

(8) Ruiz, E.; Cano, J.; Alvarez, S.; Alemany, P. *J. Am. Chem. Soc.* **1998**, *120*, 11122.

(9) Walker, N.; Stuart, D. *Acta Crystallogr.* **1983**, *A39*, 158.

(10) *SHELXTL-PC Program Package*; Siemens Analytical X-ray Instruments Inc.: Madison, WI, 1990.

10.1021/ic990878v CCC: $18.00
Published on Web 12/09/1999

Table 2. Atomic Coordinates ($\times 10^4$) and Equivalent Isotropic Displacement Coefficients ($Å^2 \times 10^3$) for $[Mn(bpm)(N_3)_2]_n$

atom	*x*	*y*	*z*	*U*(eq)[a]
Mn(1)	1773(1)	3841(1)	5308(1)	33(1)
N(11)	626(4)	6063(3)	5552(2)	37(1)
N(12)	673(4)	6665(3)	6181(2)	40(1)
N(13)	726(6)	7269(5)	6782(2)	62(1)
N(14)	4307(5)	4251(5)	6023(2)	54(1)
N(15)	5497(4)	4979(3)	5874(2)	32(1)
N(16)	6723(5)	5708(4)	5757(2)	54(1)
C(1)	2903(6)	923(5)	6517(2)	47(1)
N(1)	2747(4)	413(4)	5712(2)	42(1)
C(11)	3077(6)	−961(5)	5424(3)	51(1)
C(12)	2833(6)	−880(5)	4626(3)	58(2)
C(13)	2367(6)	594(5)	4462(2)	49(1)
N(2)	2323(4)	1403(3)	5120(2)	41(1)
N(3)	1262(5)	1573(4)	6746(2)	31(1)
C(21)	199(7)	1089(5)	7300(2)	57(1)
C(22)	−1062(7)	2155(6)	7370(3)	60(2)
C(23)	−680(6)	3274(5)	6830(2)	47(1)
N(4)	736(4)	2922(4)	6452(2)	40(1)

[a] *U*(eq) is defined as one-third of the trace of the orthogonalized $\mathbf{U}_{ij}$ tensor.

Table 3. Selected Bond Lengths (Å) and Angles (deg) for $[Mn(bpm)(N_3)_2]_n$[a]

Mn(1)−N(11)	2.216(3)	Mn(1)−N(11a)	2.254(3)
Mn(1)−N(14)	2.231(4)	Mn(1)−N(2)	2.242(3)
Mn(1)−N(16a)	2.239(4)	Mn(1)−N(4)	2.295(3)
Mn(1a)-N(11)	2.254(3)	Mn(1b)-N(16)	2.239(4)
N(1)−N(2)	1.359(4)	N(3)−N(4)	1.353(5)
N(11)−N(12)	1.193(4)	N(12)−N(13)	1.151(5)
N(14)−N(15)	1.155(5)	N(15)−N(16)	1.163(5)

N(11)−Mn(1)−N(14)	95.0(1)	N(11)−Mn(1)−N(2)	167.0(1)
N(11)−Mn(1)−N(4)	90.0(1)	N(11)−Mn(1)−N(11a)	77.1(1)
N(14)−Mn(1)−N(2)	94.3(1)	N(14)−Mn(1)−N(4)	86.1(1)
N(2)−Mn(1)−N(4)	81.5(1)	N(14)−Mn(1)−N(11a)	166.5(1)
N(2)−Mn(1)−N(11a)	95.4(1)	N(15)−N(16)−Mn(1b)	134.2(3)
N(4)−Mn(1)−N(11a)	104.6(1)	N(14)−Mn(1)−N(16a)	86.6(1)
N(11)−Mn(1)−N(16a)	102.6(1)	N(2)−Mn(1)−N(16a)	87.1(1)
N(4)−Mn(1)−N(16a)	165.9(1)	N(11a)−Mn(1)−N(16a)	84.6(1)
Mn(1)−N(2)−N(1)	124.2(2)	Mn(1)−N(2)−C(13)	131.4(3)
Mn(1)−N(11)−N(12)	125.6(2)	N(12)−N(11)−Mn(1a)	122.3(3)
Mn(1)−N(14)−N(15)	129.1(3)	Mn(1)−N(4)−N(3)	121.3(2)
N(11)−N(12)−N(13)	178.8(4)	N(14)−N(15)−N(16)	177.1(4)
Mn(1)−N(11)−Mn(1a)	102.9(1)		

[a] Symmetry codes: a = −x, 1 − *y*, 1 − *z*; *b* = 1 − *x*, 1 − *y*, 1 − *z*.

Results and Discussion

IR Spectra. In addition to the characteristic bands of bpm at 2967 cm^{-1} (ν_{C-H}) and at 1520, 1456, 1396, 1337, 1280, and 1220 cm^{-1} (pyrazolyl ring), very intense bands due to the azido groups appear at 2102 cm^{-1} (ν_{asym}), 1328 cm^{-1} (ν_{sym}), and 602 and 614 cm^{-1} (δ). The peak at about 2100 cm^{-1} was slightly broad.

Description of the Structure. An ORTEP plot of the basic unit and a view of the one-dimensional chains of $[Mn(bpm)(N_3)_2]_n$ are shown in Figure 1 and Figure 2. The crystal structure consists of neutral chains of Mn(II) ions alternately linked by two EO (end-on) parts [Mn(1)−N(11) 2.216(3), Mn(1)−N(11a), 2.254(3) Å] and two EE (end-to-end) parts [Mn(1)−N(14) 2.231(4), Mn(1)−N(16a), 2.239(4) Å]. Coordination around the manganese atoms consists of N atoms from bpm ligands in the form of a cis distorted octahedron. The EO bridging azides, which are quasi-linear [N(11)−N(12)−N(13) 178.8(4)°], deviate slightly from the plane, and their angles are slightly larger than the value reported for $[Mn(bipy)(N_3)_2]_n$ [176.6(8)°].[4a] The Mn(1)−N(11)−Mn(1a) angle in the EO mode is 102.9(1)°,

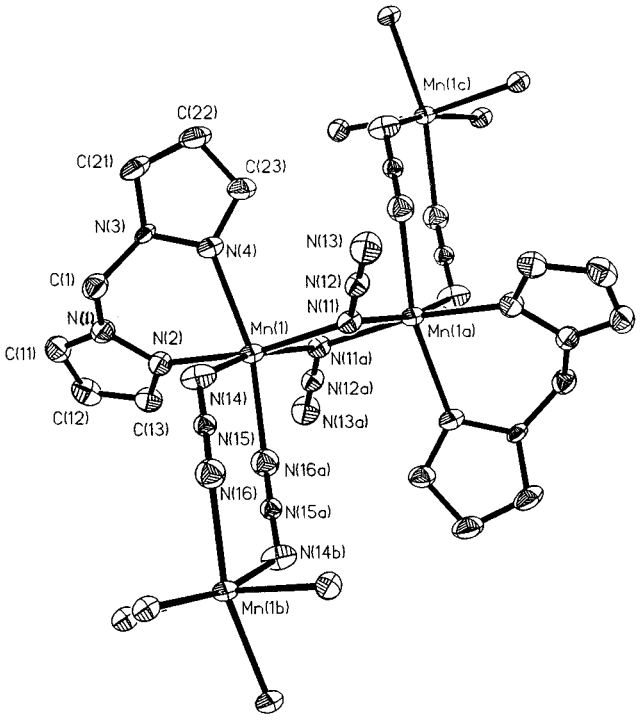

Figure 1. ORTEP drawing (30% thermal ellipsoids) of $[Mn(bpm)(N_3)_2]_n$ with the atom-labeling scheme.

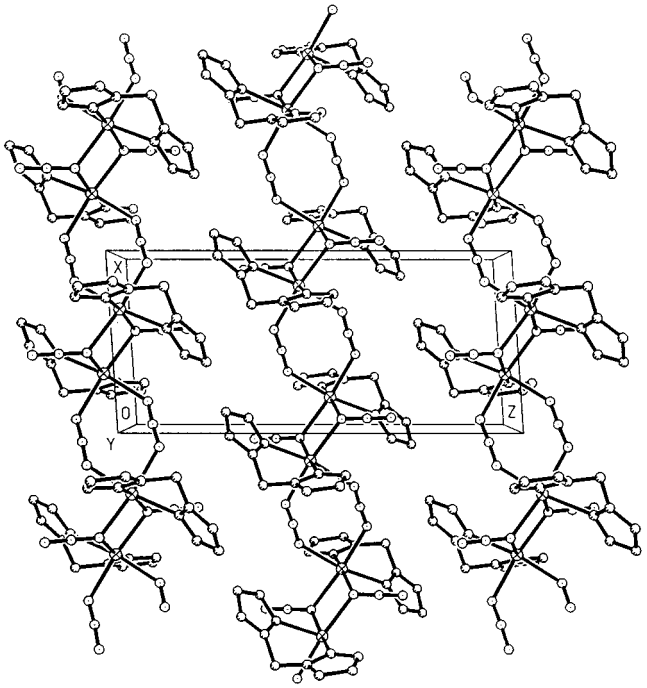

Figure 2. View of the chains (30% thermal ellipsoids) of $[Mn(bpm)(N_3)_2]_n$ in the unit cell.

similar to the results (100−105°) obtained for this kind of bridging ligand[2,7] and larger than the value for $[Mn(bipy)(N_3)_2]_n$ [101.0(2)°]. The two Mn−N−N bond angles related to the end-on azido bridges are asymmetrical [Mn(1)−N(11)−N(12) 125.6(2)° and Mn(1a)−N(11)−N(12) 122.3(3)°]. The Mn(1)···Mn(1a) distance is 3.496(4) Å (end-on azido bridges), and the Mn(1)···Mn(1b) distance is 5.484(3) Å (end-to-end azido bridges). For the EE bridges, the Mn(1)−N(14)−N(15) angle is 129.1(3)° and the Mn(1b)−N(16)−N(15) angle is 134.2(3)°. The torsion τ angle between the mean plane of Mn(1)−N(14)−N(15)−N(16) and Mn(1b)−N(16)−N(15)−

Table 4. Selected Structural and Magnetic Parameters for the Alternating One-Dimensional Chain System

		M···M (Å)					J (cm^{-1})			
compd	M−N−M (deg)	EO	EE	M−N−N (deg)	τ (deg)	δ (deg)	EE	EO	α	ref
$[Mn(bipy)(N_3)_2]_n$	101.0	3.455	5.343	131.1 127.3	41.1	22.7	−11.9	10.0	1.2	4a[a]
							−6.3	2.5	2.5	4d[a]
$[Mn(bpm)(N_3)_2]_n$	102.9	3.496	5.484	129.1 134.2	41.1	20.5	−63.7	15.7	4.2	this work
$[Ni(bipy)(N_3)_2]_n$	101.5	3.248	5.117	118.2 129.9		35.2	−2.6	26	0.1	4d
$[Ni(dmen)(N_3)_2]_n$	100.5 101.2 102.9	3.350 3.272	5.247	130.9 132.9		8.4	−120	20 37	6 3.2	12

[a] The same compound.

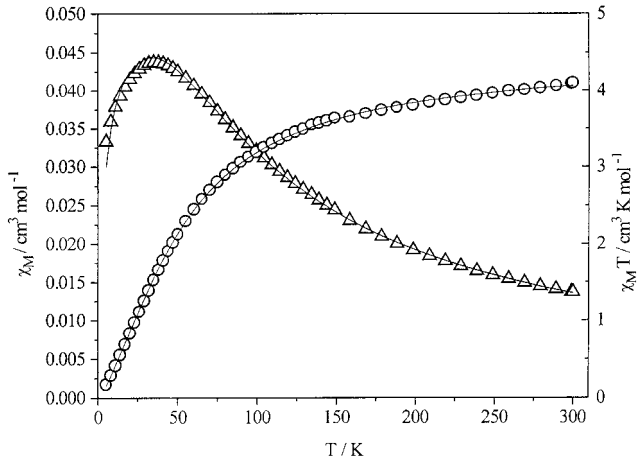

Figure 3. Plots of $\chi_M T$ (○) and χ_M (△) of $[Mn(bpm)(N_3)_2]_n$ versus T. Solid lines represent the best theoretical fits.

N(14) for a chair configuration[4c] is 41.1°, and the dihedral δ angle between the least-squares plane defined for the six nitrogen atoms of the EE bridging azides and the N(14)−Mn(1)−N(16a) plane[4c] is 20.5°.

Magnetic Properties. Variable-temperature magnetic susceptibility measurements were performed on a polycrystalline sample in the range 300−5 K with a SQUID magnetometer, and the results are shown in Figure 3. The applied magnetic field was 3000 G. For the complexes, the χ_M values increase as the temperature decreases, reaching a maximum at about 35 K, and then decrease on cooling to 5 K. The $\chi_M T$ value at room temperature is 4.10 cm^3·K·mol^{-1}, which is smaller than the expected value for an uncoupled manganese(II) ion and is close to the value observed for $[Mn(bipy)(N_3)_2]_n$.[4a] The magnetic susceptibility data were interpreted on the basis of a theoretical model for the alternating ferromagnetic−antiferromagnetic $S = {}^5/_2$ chain. In addition, to obtain the satisfactory results at low temperature, a Weiss constant (Θ) was introduced to account for interchain interactions in the solid state.[11] Following the model and fixing g to the expected value of 2.0 for manganese(II), we obtained a very satisfactory fit of the data at 5−300 K: $J_1 = 15.7$ cm^{-1}, $J_2 = -67.6$ cm^{-1}, $\Theta = -3$ K; R is defined as $\sum[(\chi_M T)^{obs} - (\chi_M T)^{calc}]^2/\sum[(\chi_M T)^{obs}]^2$ and is found to be 3.5×10^{-4}.

It is very interesting to compare the structures and magnetic properties with those reported for $[Mn(bipy)(N_3)_2]_n$ which is structurally analogous. For both complexes $[Mn(bpm)(N_3)_2]_n$ and $[Mn(bipy)(N_3)_2]_n$, given the different Mn−N−Mn angles (102.9 and 101.0°, respectively) for the EO coordination mode, the J_1 value of 15.7 cm^{-1} for the former is greater than the J_1 value for the latter (13.8 cm^{-1}). On the other hand, to consider the relation between δ and the superchange J_2 parameter for the EE coordination model in which the torsion angles are the same (41.1°), the antiferromagnetic coupling should be decreased for the larger δ value ($J_2 = -67.6$ cm^{-1}, $\delta = 20.5°$ for the former; $J_2 = -17.0$ cm^{-1}, $\delta = 22.7°$ for the latter). The results compared with other experimental values for alternating-chain complexes are summarized in Table 4. The α value, defined as the alternation parameter, $[|J_{EE}/J_{EO}|]$, indicates that the difference in the magnitudes of the magnetic interactions through azido ligands is large.

In conclusion, the relationships presented may be deduced from the structural data and the magnetic properties available: two end-on bridging azido ligands favor ferromagnetic interaction, and a relation between J and δ exists where larger δ is more effective in transfering ferromagnetic interactions, which is consistent with the results based on the density functional approach.[8] The antiferromagnetic interactions should decrease as the torsion angles increase, which indicates that the torsion angle is the factor controlling the antiferromagnetic coupling and which is in excellent agreement with the EHMO results.[4a]

Acknowledgment. This work was supported by the National Natural Science Foundation of China. We thank S. Y. Fan (Beijing Institute of Physics, Chinese Academy of Sciences) for measuring the magnetic data.

Supporting Information Available: Tables listing detailed experimental crystallographic data, non-hydrogen positional parameters, thermal parameters, bond lengths and angles, least-squares planes, and magnetic susceptibility data for $[Mn(bpm)(N_3)_2]_n$. This material is available free of charge via the Internet at http://pubs.acs.org.

IC990878V

(11) Bertrand, J. A.; Caine, D. *J. Am. Chem. Soc.* **1964**, *86*, 2298.
(12) Rabis, J.; Monfort, M.; Resino, I.; Solans, X.; Rabu, P.; Maingot, F.; Drillon, M. *Angew. Chem., Int. Ed. Engl.* **1996**, *35*, 2520.